Charge Exchange and Threshold Effect in the Energy Loss of Slow Projectiles

R. Cabrera-Trujillo, John R. Sabin, Y. Öhrn, and E. Deumens

Quantum Theory Project, Departments of Physics and Chemistry, University of Florida, Gainesville, Florida 32611-8435

(Received 19 November 1999)

In this Letter, we study charge exchange and energy loss of protons, taking into account the dynamics of both nuclei and electrons during the collision with atomic hydrogen, helium, and neon targets. We obtain the nuclear and electronic contributions to the energy loss as well as the charge exchange probability, and the total cross section for charge exchange. We find a low-energy threshold in the electronic energy loss due to the quantization of excited states. We find that the electronic stopping cross section is not proportional to the velocity of the projectile at very low velocities (energies), as is predicted by electron gas theory. This confirms recent experimental results.

PACS numbers: 34.50.Bw, 34.70.+e

Theoretical studies, based either on the stopping of a point charge in a free-electron gas [1,2] or on the quasi-free-electron flux between two colliding atoms [3], predict that the electronic stopping power of light ions at low speeds is approximately proportional to the projectile speed with intercept at the origin. However, it has been observed experimentally that the stopping power for low-energy particles is not always proportional to projectile speed [4,5]. Furthermore, the slowing down of protons in insulators is influenced by the energy gap; hence, a threshold effect could be expected [6]. Recently, in a measurement of protons on bulk LiF no evidence for influence of the band gap on stopping power was found [7], while, in a grazing incidence experiment on the same system [8], there were indications of threshold behavior which was attributed to charge exchange.

For inelastic processes at low to intermediate energies where the interaction time is long enough to allow for charge exchange, excitation, and ionization, there is no satisfactory theory. Although there have been some studies of projectile charge exchange in the energy loss process, they are based on a dielectric [9] or statistical [10] description. From the point of view of *ab initio* theory, there have been only a few attempts to study the dynamics of energy loss for a bare particle (without charge exchange) [11,12], and for one active electron [13].

Our goal has been to develop a single consistent scheme which can treat all processes that take place over the full range of projectile speeds by implementing a time-dependent approach to molecular dynamics called electron nuclear dynamics (END) [14,15]. The END method is based on the time-dependent variational principle (TDVP). It produces an approximation to the time-dependent Schrödinger equation for the system, including nuclear and electronic degrees of freedom and their interaction. The END method uses a molecular description of the system, i.e., a single determinantal, spin-unrestricted, electronic wave function centered on the dynamically changing nuclear positions to describe the system as a whole. The TDVP produces a set of coupled first-order differential equations for the time evolution of the parameters of the wave function. This approximation is implemented in the ENDYNE code [16].

Early applications of the END theory include the analysis of protons colliding with hydrogen atoms [14], hydrogen molecules [17], helium atoms [18], methane molecules [19], oxygen atoms [20], and water molecules [21]. Most of this work has been done for collision energies ranging from a fraction of an eV to several tens of eV, and mainly in order to describe chemical reactions. Recently, we have applied the method to the analysis of direct differential cross section for H^+, H, and He projectiles colliding with He and Ne targets at projectile energies of a few keV [22], giving us confidence in the applicability of the model to the analysis of atomic collisions at higher energies. Here we are interested in projectile energies ranging from a few eV to several keV with particular attention to charge exchange properties and energy loss of protons on H, He, and Ne.

For each impact parameter, we calculate the deflection angle of the projectile, the final projectile charge (from the Mulliken population analysis, i.e., we analyze the charge density in terms of the atomic orbitals centered on the various atoms and obtain a measure of how the total charge density is distributed between the various centers after the collision has taken place) [23], and the final energy (kinetic and electronic energy) for the projectile. Specifically, we have considered proton projectiles with initial energies ranging from 10 eV to 300 keV. For the targets we have used basis sets consisting of $[6s3p2d/4s3p2d]$ for H, $[9s5p2d/6s5p2d]$ for He, and a $[10s5p2d/4s3p2d]$ for Ne atoms [24], with the addition of three s-type and two p-type diffuse orbitals for a better description of the wave function's tail. For the projectile, we use a $[5s2p/3s2p]$ basis set [24] traveling with the projectile. For high energies, only twenty values of the impact parameter were considered due to the smoothness of the behavior of the charge exchange as a function of the impact parameter. For lower energies, the probabilities for charge exchange display an oscillatory behavior for the case of hydrogen targets (see Fig. 1), thus a more compact grid of impact parameters (40 values) was needed. All impact parameter values lie between 0.0 and 20 a.u. The trajectories started

 0031-9007/00/84(23)/5300(4)$15.00

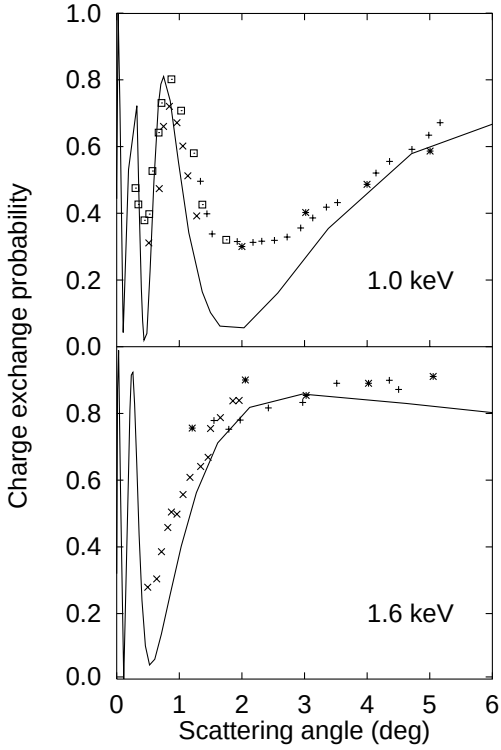

FIG. 1. Charge exchange probability as a function of the scattering angle for protons colliding with hydrogen atoms at 1.0 and 1.6 keV in the laboratory frame. The experimental data $\times, +$ were taken from [25], and $*$ from [26].

with the projectile 30 a.u. from the target and finish with the projectile 30 a.u. past the target.

In Fig. 1, we compare the present END results for the charge exchange between atomic hydrogen targets and proton projectiles with experimental data [25,26]. In the two cases considered, the projectile has initial energy of 1.0 and 1.6 keV, in the range where we expect charge exchange to be most important. For lower energies, the charge oscillations (which we identify with quasimolecule states) are more pronounced, which makes the final charge of the projectile more screened, depending on the impact parameter (or scattering angle). We attribute the discrepancies between theory and experiment to the limited angular resolution in the experiments. The overall agreement between theory and experiment, principally the agreement of the position of the minima and maxima of the charge exchange probability, gives us confidence in the description of the dynamics of the collision in the low-energy region.

Integrating the charge exchange probabilities over all the impact parameters, one obtains the total cross section for charge exchange, which is shown in Fig. 2, as a function of the projectile energy for protons colliding with atomic hydrogen, helium, and neon targets, and compare with experimental data [27–29]. For protons colliding with atomic hydrogen we see fair agreement with experiment, principally in the low-energy region ($E_p < 25$ keV). For higher energies, we note that the ionization channel is not

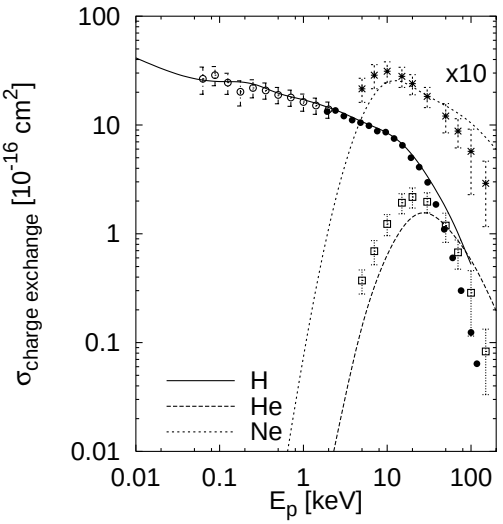

FIG. 2. Total cross section for charge exchange of protons as a function of the projectile energy for collisions with atomic hydrogen, helium, and neon targets. The experimental data are from $\circ$ [27], $\bullet$ [28], and ($\square$, $*$) [29].

taken explicitly into account in these calculations. If it was, the charge exchange cross section would be lower than the present results, in better agreement with the experiment. For protons colliding with helium and neon, the results show an overall agreement with experiment, principally at the maximum of the total charge exchange cross section.

From the final speed of the projectile, we determine the kinetic energy loss and calculate the stopping cross section by means of

$$S_x(v) = 2\pi \int_0^\infty \Delta E_x(b) b \, db \,, \tag{1}$$

where the x labels the electronic (e), nuclear (n), or total (t, electronic + nuclear) contribution to the energy loss, ΔE. In Fig. 3, we show the total, electronic, and nuclear stopping cross sections for protons colliding with atomic hydrogen from energies ranging from a few eV to hundreds of keV, and compare with the experimental data available [30–34]. We see fair agreement between theory and experiment, principally for energies from the maximum of the stopping curve and higher. However, for lower energies, there are some discrepancies, due principally to the charge exchange processes, since the lower the energy the more screened is the projectile (see Fig. 2). Also, we note that our results were obtained for atomic hydrogen, while the experimental data were obtained for the hydrogen molecule, and thus contain chemical bond effects.

In Figs. 4 and 5, we show the results for protons colliding with atomic helium and neon targets as a function of the projectile energy, and compare with experimental data [30,33,35,36]. From these figures, we see fair agreement between theory and experiment, even though for high energies the ionization channel is not explicitly open. If it were open, we would expect to lower our results.

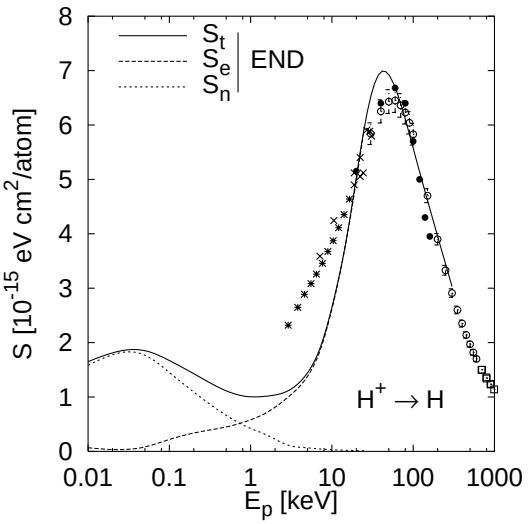

FIG. 3. Stopping cross section for proton incident on atomic hydrogen as a function of the projectile energy. The lines labeled with END are the results of this work with electronic (e), nuclear (n), and total (t, nuclear + electronic) contribution. The experiments are from $*$ [30], $\circ$ [33], $\bullet$ [32], $\square$ [31], and $\times$ [34].

From Figs. 3, 4, and 5, it seems apparent that there is a low velocity threshold below which there is no electronic stopping cross section. This threshold is a consequence of the quantum behavior of the momentum transfer and the molecular states of the system during the collision.

For a binary collision, the minimum momentum transferred during a collision, obtained through energy conservation, is given by [37]

$$q_{\min} = \frac{\mu v}{\hbar}\left[1 - \sqrt{1 - \frac{2(E_k - E_{k_0})}{\mu v^2}}\right], \qquad (2)$$

where μ is the reduced mass of the projectile-target system, v is the projectile incoming speed, and $E_k - E_{k_0}$ is the electronic energy absorbed by the target (transition energy from the initial state k_0 to the final state k). In order that this momentum transfer be enough for an electronic transition, it is necessary that

$$\frac{\hbar^2 q_{\min}^2}{2m_e} \geq (E_k - E_{k_0}). \qquad (3)$$

Solving for the projectile incoming energy in the laboratory system, one finds

$$E_p \geq \frac{\mu^2}{4M_1 m_e}(E_k - E_{k_0})\left[1 + \frac{m_e}{\mu}\right]^2, \qquad (4)$$

where M_1 is the projectile mass. For helium, the lowest transition is $1s^2(^1S_o) \rightarrow 1s2s(^3S)$, with an excitation energy of 18.7 eV, as calculated with ENDYNE (19.72 eV [38]). Therefore, the threshold for the electronic stopping cross section for a proton colliding with helium should be at approximately $E_p = 8$ keV, which is close to the result shown in Fig. 4. For the case of neon, the lowest excitation is $1s^2 2s^2 2p^6(^1S_o) \rightarrow 1s^2 2s^2 2p^5(^2P_{3/2})3s^1$ with an excitation energy of 14.9 eV, as calculated with ENDYNE (16.5 eV [38]), such that the projectile energy threshold is expected to be near $E_p = 7$ keV. Note that Eq. (4) has been obtained assuming that there are no charge exchange processes involved during the collision. For helium and neon atoms, this is mostly the case, since we have a small charge exchange cross section (see Fig. 2). The hydrogen target is more complicated due to the charge exchange processes, and the quasimolecular states formed during the collision.

We conclude that for low energies the electronic stopping cross section is not proportional to the projectile

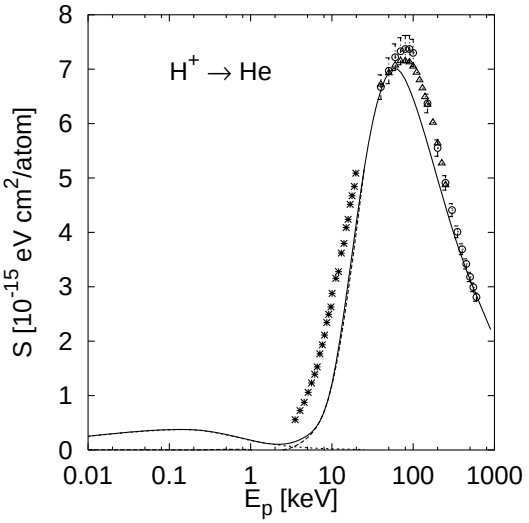

FIG. 4. Stopping cross section for proton incident on atomic helium as a function of the projectile energy. The labels are the same as in Fig. 3. The experimental data $\triangle$ is from [35]. Note the threshold in the electronic energy loss at low energies.

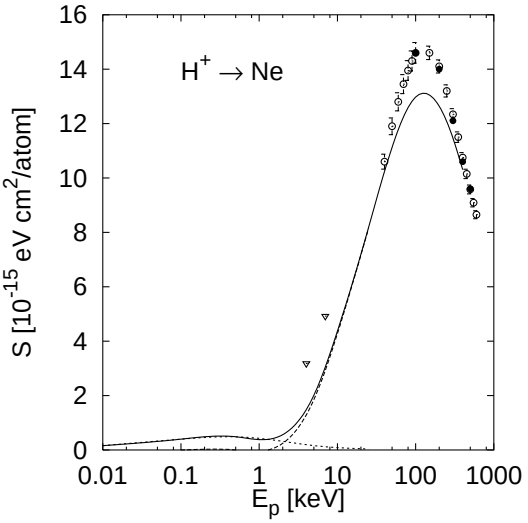

FIG. 5. Stopping cross section for proton incident on atomic neon as a function of the projectile energy. The labels are the same as in Fig. 3. The experimental data $\triangledown$ is from [36]. Note the threshold in the electronic energy loss at low energies.

velocity and shows a threshold which is a consequence of the quantization of the target energy levels. Also, we have shown the importance of taking into account the charge exchange processes for low energies. We hope this work may stimulate further experimental and theoretical work on low-energy stopping cross sections.

This work was supported in part by CONACyT-Mexico to R. C. T., by NSF (Grant No. CHE-9732902), and by ONR (Grant No. N0014-00-1-0197).

[1] E. Fermi and E. Teller, Phys. Rev. **72**, 399 (1947).
[2] J. Lindhard and M. Scharff, K. Dan. Vidensk. Selsk. Mat. Fys. Medd. **28**, 8 (1954).
[3] O. B. Firsov, Sov. Phys. JETP **36**, 1076 (1959).
[4] R. Golser and D. Semrad, Phys. Rev. Lett. **66**, 1831 (1991).
[5] M. Kimura, Phys. Rev. A **47**, 2393 (1993).
[6] D. Semrad, Phys. Rev. A **33**, 1646 (1986).
[7] K. Eder *et al.*, Phys. Rev. Lett. **79**, 4112 (1997).
[8] C. Auth, A. Mertens, H. Winter, and A. Borisov, Phys. Rev. Lett. **81**, 4831 (1998).
[9] A. Arnau, M. Peñalba, P. M. Echenique, and F. Flores, Nucl. Instrum. Methods Phys. Res., Sect. B **69**, 102 (1992).
[10] P. Sigmund, Nucl. Instrum. Methods Phys. Res., Sect. B **69**, 113 (1992).
[11] G. Schiwietz, Phys. Rev. A **42**, 296 (1990).
[12] P. L. Grande and G. Schiwietz, Phys. Rev. A **44**, 2984 (1991).
[13] P. L. Grande, G. Schiwietz, G. M. Sigaud, and E. C. Montenegro, Phys. Rev. A **54**, 2983 (1996).
[14] E. Deumens, A. Diz, H. Taylor, and Y. Öhrn, J. Chem. Phys. **96**, 6820 (1992).
[15] E. Deumens, A. Diz, R. Longo, and Y. Öhrn, Rev. Mod. Phys. **66**, 917 (1994).
[16] E. Deumens *et al.*, "ENDYNE version 2.7 Software for Electron Nuclear Dynamics," Quantum Theory Project, University of Florida, 1998.
[17] J. A. Morales, A. C. Diz, E. Deumens, and Y. Öhrn, J. Chem. Phys. **103**, 9968 (1995).
[18] R. Longo, E. Deumens, and Y. Öhrn, J. Chem. Phys. **99**, 4554 (1993).
[19] D. Jacquemin, J. A. Morales, E. Deumens, and Y. Öhrn, J. Chem. Phys. **107**, 6146 (1997).
[20] M. Hedström, E. Deumens, and Y. Öhrn, Phys. Rev. A **57**, 2625 (1998).
[21] M. Hedström, J. A. Morales, E. Deumens, and Y. Öhrn, Chem. Phys. Lett. **279**, 241 (1997).
[22] R. Cabrera-Trujillo, J. R. Sabin, Y. Öhrn, and E. Deumens, Phys. Rev. A **61**, 032719 (2000).
[23] R. S. Mulliken, J. Chem. Phys. **23**, 1833 (1955).
[24] T. H. Dunning, J. Chem. Phys. **90**, 1007 (1989).
[25] J. C. Houver, J. Fayeton, and M. Barat, J. Phys. B, At. Mol. Phys. **7**, 1358 (1974).
[26] H. F. Helbig and E. Everhart, Phys. Rev. **140**, 1715 (1965).
[27] M. W. Gealy and B. Van Zyl, Phys. Rev. A **36**, 3091 (1987).
[28] G. W. McClure, Phys. Rev. **148**, 47 (1966).
[29] M. E. Rudd *et al.*, Phys. Rev. A **28**, 3244 (1983).
[30] R. Golser and D. Semrad, Nucl. Instrum. Methods Phys. Res., Sect. B **69**, 18 (1992).
[31] G. Reiter, N. Kniest, E. Pfaff, and G. Clausnitzer, Nucl. Instrum. Methods Phys. Res., Sect. B **44**, 399 (1990).
[32] S. K. Allison, J. Cuevas, and M. Garcia-Munoz, Phys. Rev. **127**, 792 (1962).
[33] H. K. Reynolds, D. N. Dunbar, W. A. Wenzel, and W. Whaling, Phys. Rev. **92**, 742 (1953).
[34] J. A. Phillips, Phys. Rev. **90**, 532 (1953).
[35] J. T. Park and E. J. Zimmerman, Phys. Rev. **131**, 1611 (1963).
[36] A. Schiefermüller, R. Golser, R. Stohl, and D. Semrad, Phys. Rev. A **48**, 4467 (1993).
[37] M. Inokuti, Rev. Mod. Phys. **43**, 297 (1971).
[38] R. F. Bacher and S. Goudsmit, in *Atomic Energy States*, edited by F. K. Richtmyer (McGraw-Hill, New York, 1932).